π plasmons in carbon nanotube bundles

M. F. Lin
Department of Physics, National Cheng Kung University, Tainan 70101, Taiwan, Republic of China

D. S. Chuu
Electrophysics Department, National Chiao Tung University, Hsinchu 30050, Taiwan, Republic of China

(Received 20 November 1997)

The π-electronic collective excitations (π plasmons) in carbon nanotube bundles are studied within the linear-response approximation. The intertube Coulomb interactions significantly affect the electronic excitations, so that the π plasmons in nanotube bundles are quite different from those in a single nanotube. The π plasmons strongly depend on the direction and magnitude of the transferred momentum. They clearly exhibit the anisotropic behavior. Moreover, the π plasmon frequencies are lower for bundles made up of larger nanotubes. [S0163-1829(98)04815-2]

Iijima[1] recently reported observation of carbon nanotubes, which are graphite sheets rolled up in a cylindrical form. A carbon nanotube consists of either a single-shell nanotube or multishell nanotubes with a radius 10–150 Å. Such a quasi-one-dimensional system has motivated many studies on the electronic structures[2–7] and excitations.[8–20] When carbon nanotubes are packed together, they would form a three-dimensional (3D) system, a carbon nanotube bundle (CNB). CNB's, which are made up of different multi-shell[21,22] or single-shell[23] nanotubes, have been produced. It is currently possible to produce a uniform CNB composed of the same single-shell nanotubes.[24,25] Moreover, carbon nanotubes, with armchair structures, are found to be located in accord with a 2D triangular lattice. Metallic atoms and molecules could be further intercalated into CNB's. Experimental measurements demonstrate that the intercalation has a strong effect on conductivity[26] and the Raman spectrum.[27] In this work we mainly study the π-electronic collective excitations (π plasmons) of a uniform CNB by evaluating the longitudinal dielectric function (ϵ). Their dependence on the transferred momentum [$\mathbf{q}_t=(q,\mathbf{q}_\perp)$] and the nanotube radius (r) is investigated.

We use the tight-binding model[4] to calculate the π band formed by $2p_z$ orbitals. The π-electronic response function of a uniform CNB is evaluated within the linear-response approximation.[28] Carbon nanotubes are coupled by the Coulomb interactions among electrons. The intertube Coulomb coupling would significantly affect the characteristics of the π plasmons. A single carbon nanotube is predicted to exhibit the decoupled π plasmons of different angular momenta (L).[17–20] However, the π plasmons in CNB's are associated with the superposition of the various L-mode excitations of all nanotubes. Our study shows that the π plasmons strongly depend on the magnitude and the direction of the transferred momenta as well as the nanotube radius. The calculated results could be verified from the measurements of the momentum-dependent electron-energy-loss spectrum (EELS).

A single-layer nanotube could be regarded as a rolled-up graphite sheet. Its structure is uniquely characterized by a 2D lattice vector $\mathbf{R}_x=m\mathbf{a}_1+n\mathbf{a}_2$, where $\mathbf{a}_1$ and $\mathbf{a}_2$ are primitive lattice vectors of a graphite sheet and m and n are integers.[29] The radius and the chiral angle of a (m,n) nanotube are

$$r=\frac{|\mathbf{R}_x|}{2\pi}=\frac{b\sqrt{3(m^2+mn+n^2)}}{2\pi}$$

and

$$\theta=\tan^{-1}\frac{-\sqrt{3}n}{(2m+n)},$$

respectively.[14] $b=1.42$ Å is the C-C bond length. Armchair (m,m) nanotubes, as found in a uniform CNB,[24,25] are taken for a model study. The π band is calculated from the nearest-neighbor tight-binding Hamiltonian.[4] The wave function and the energy dispersion are denoted, respectively, by Ψ^h_{J,k_v} and E^h_{J,k_v} $(h=v,c)$.[20,29] k_y is the wave vector along the tubular axis and J is the angular momentum. $h=v$ $(h=c)$ corresponds to the occupied valence band (the unoccupied conduction band). The π-electronic excitations [Eq. (6)] are the interband excitations from the v band to the c band or vice versa.

We consider a uniform CNB in which the same single-shell nanotubes are packed into a triangular lattice with the lattice constant d $(=3.15$ Å$)$.[24] The nanotube number per area is $N_a=2/\sqrt{3}(2r+d)$.[2] The tight-binding wave function of the nanotube bundle is

$$|\alpha\rangle=|\mathbf{k}_\perp;J,k_y,h\rangle$$
$$=C\sum_{\mathbf{R}_{\perp,m}}\exp(i\mathbf{k}_\perp\cdot\mathbf{R}_{\perp,m})\Psi^h_{J,k_y}(y,\mathbf{r}_\perp-\mathbf{R}_{\perp,m}), \quad (1)$$

where C is the normalization factor and $\mathbf{R}_{\perp,m}$ is the 2D lattice vectors. $\perp$ represents the direction perpendicular to the tubular axis, for example, $\mathbf{k}_\perp$ is perpendicular to k_y.

The dielectric function of a CNB is calculated within the linear-response approximation. The bundle is assumed to be perturbed by the time-dependent potential $V^{\rm ex}(q,\mathbf{q}_\perp,\omega)$. The π electrons on all nanotubes would screen this external field,

which thus causes the charge fluctuations. The induced potential due to the induced charges is directly obtained from the Poisson equation

$$V^{\rm in}(q,\mathbf{q}_\perp,\omega)=V(q,\mathbf{q}_\perp)n^{\rm in}(q,\mathbf{q}_\perp,\omega). \tag{2}$$

$V(q,\mathbf{q}_\perp)=4\pi e^2/(q^2+\mathbf{q}_\perp^2)$ is the Fourier component of the 3D bare Coulomb interaction. The approximation, which is similar to the self-consistent-field approach,[28] is used to evaluate the induced charge density. Within the linear-response approximation we get

$$n^{\rm in}(q,\mathbf{q}_\perp,\omega)=\chi(q,\mathbf{q}_\perp,\omega)V^{\rm eff}(q,\mathbf{q}_\perp,\omega) \tag{3}$$

and

$$\chi(q,\mathbf{q}_\perp,\omega)=2\sum_{\alpha,\alpha'}|\langle\alpha'|e^{iqy}e^{i\mathbf{q}_\perp\cdot\mathbf{r}_\perp}|\alpha\rangle|^2 \times\frac{f^0(E_{\alpha'})-f^0(E_\alpha)}{E_{\alpha'}-E_\alpha-(\omega+i\Gamma)}. \tag{4}$$

The factor of 2 accounts for the spin degeneracy. f^0 is the Fermi-Dirac function. Γ is the energy width due to the deexcitation mechanisms. $E_\alpha=E^h_{J,k_y}$ is the energy dispersion of each nanotube. The induced potential is proportional to the effective potential, in which the coefficient is the response function $\chi(q,\mathbf{q}_\perp,\omega)$. The effective potential is the sum of the external potential and the induced potential, so the dielectric function defined by $V^{\rm ex}/V^{\rm eff}$ is

$$\epsilon(q,\mathbf{q}_\perp,\omega)=\epsilon_0-V(q,\mathbf{q}_\perp)\chi(q,\mathbf{q}_\perp,\omega). \tag{5}$$

$\epsilon_0(=2.4)$ (Ref. 20) is the background dielectric constant.

The response function of the nanotube bundle is the superposition of those of separate nanotubes. By a detailed analysis, the response function is reduced to

$$\chi(q,\mathbf{q}_\perp,\omega) =2N_a\sum_{J,J',k_y,h,h'}|\langle J',k_y+q,h'|e^{iqy}e^{i\mathbf{q}_\perp\cdot\mathbf{r}_\perp}|J,k_y,h\rangle|^2 \times\frac{f^0(E^{h'}_{J',k_y+q})-f^0(E^h_{J,k_y})}{E^{h'}_{J',k_y+q}-E^h_{J,k_y}-(\omega+i\Gamma)}. \tag{6}$$

The above summation is only related to the states of an isolated nanotube. Hence $\chi(q,\mathbf{q}_\perp,\omega)$ of a CNB is associated with that $[\chi(q,L,\omega)]$ of a single-shell nanotube.[20] The square of the matrix element in Eq. (6) is further evaluated from the series expansion

$$\exp(i\mathbf{q}_\perp\cdot\mathbf{r}_\perp)=\sum_L\frac{(iq_\perp r)^L}{L!}\left(\frac{e^{i\phi'}+e^{-i\phi'}}{2}\right)^L, \tag{7}$$

where ϕ' is the azimuthal angle and L is the transferred angular momentum. Finally, the dielectric function is approximately given by

$$\epsilon(q,\mathbf{q}_\perp,\omega)\approx\epsilon_0-\frac{8\pi^2e^2N_a}{(q_\perp^2+q^2)}\left\{\left[1+\frac{r^4q_\perp^4}{16}+\frac{r^8q_\perp^8}{4096}\right]\times\chi(q,L=0,\omega)+\left[\frac{r^2q_\perp^2}{2}+\frac{r^6q_\perp^6}{128}\right]\chi(q,L=1,\omega) +\left[\frac{r^4q_\perp^4}{32}+\frac{r^8q_\perp^8}{4608}\right]\chi(q,L=2,\omega) +\frac{r^6q_\perp^6}{1152}\chi(q,L=3,\omega) +\frac{r^8q_\perp^8}{73\,728}\chi(q,L=4,\omega)\right\}. \tag{8}$$

Such an approximation is good except that $q_\perp r$ is very large. Equation (8) could be generalized to describe a CNB threaded by magnetic flux ϕ if $\chi(q,L,\omega)$ is changed into $\chi(q,L,\phi,\omega)$. Moreover, it is suitable for other bundles, e.g., intercalated CNB's (Refs. 26 and 27) and electron-gas cylinder bundles.

The dielectric function markedly depends on the direction and the magnitude of $\mathbf{q}_t$. The EELS is thus expected to exhibit the anisotropic behavior. The polar angle between $\mathbf{q}_t$ and the axial direction is specified by θ. The two simple cases $\mathbf{q}_\perp=0$ ($\theta=0°$) and $q=0$ ($\theta=90°$) are discussed. The dielectric function without $\mathbf{q}_\perp$ is

$$\epsilon(q,\omega)=\epsilon_0-\frac{8\pi^2e^2N_a}{q^2}\chi(q,L=0,\omega). \tag{9}$$

When the external electric field is parallel to the axial direction, the dielectric response of the CNB is the superposition of the $L=0$ excitations of all carbon nanotubes. Equation (9) is similar to that $[\epsilon(q,L=0,\omega)=\epsilon_0-4\pi e^2I_{L=0}(qr)K_{L=0}(qr)\chi(q,L=0,\omega)]$ of a single-shell nanotube.[20] $I_{L=0}$ ($K_{L=0}$) is the first (second) kind of modified Bessel function of order $L=0$. However, the different Coulomb interactions is the main difference between them. On the other hand, for the $q=0$ case, the dielectric function at small $\mathbf{q}_\perp$ is

$$\epsilon(\mathbf{q}_\perp,\omega)\approx\epsilon_0-4\pi^2e^2r^2N_a\chi(q=0,L=1,\omega) -\frac{1}{4}\pi^2e^2r^4q_\perp^2N_a\chi(q=0,L=2,\omega). \tag{10}$$

The dielectric response at the long-wavelength limit ($\mathbf{q}_\perp\rightarrow0$) is the superposition of the $L=1$ excitations, which contrasts greatly with that in the $\mathbf{q}_\perp=0$ case [Eq. (9)]. This result further illustrates that the CNB is an anisotropic system.

The EELS, defined as $\mathrm{Im}[-1/\epsilon(q,\mathbf{q}_\perp,\omega)]$, is calculated at $\Gamma=0.5$ eV for the study of the π plasmon. Figure 1 presents the EELS of the (5,5) nanotube bundle at $\theta=0°$ and various q_t's. There exists a very pronounced peak in each of the spectra, which is identified as the π plasmon. This plasmon is due to the superposition of the $L=0$ collective excitations of all nanotubes [Eq. (9)]. The π plasmon frequency (w_p) clearly increases with the transferred momentum, i.e., the π plasmons exhibit the strong momentum dependence. In addition to the transferred momenta, the EELS, as seen in

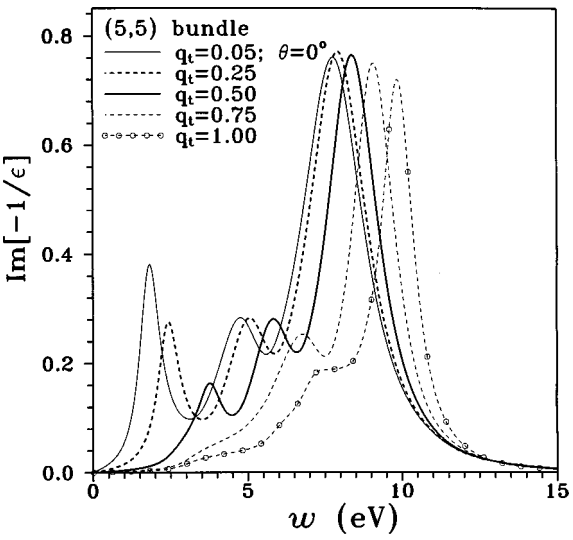

FIG. 1. The EELS of the (5,5) bundle is calculated at various transferred momenta (q_t) along the tubular axis ($\theta=0°$). The unit of q_t is $Å^{-1}$ henceforth.

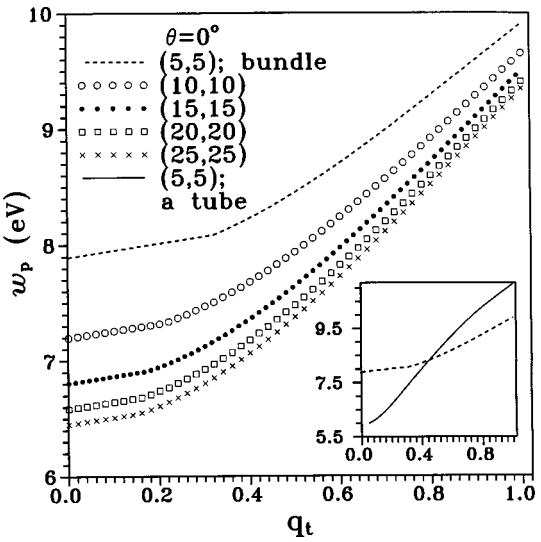

FIG. 3. The momentum dependence of the π plasmon frequency is shown for various nanotube bundles at $\theta=0°$. The $L=0$ plasmon frequency of a single (5,5) nanotube is also shown in the inset for comparison.

Fig. 2, changes with the nanotube radius. For a bundle with smaller nanotubes, the EELS intensity is stronger and the π plasmon frequency is higher. That the dielectric response of CNB's [Eq. (6)] is proportional to the nanotube density is the main reason. Also notice that a single nanotube exhibits a similar π plasmon peak in the $L=0$ excitation spectrum, but such a peak would vanish at the long-wavelength limit $q \to 0$ (inset in Fig. 3).[20] The long-wavelength collective excitations in the CNB, which correspond to the plasma oscillations along the axial direction, are indicated to be mainly supported by the intertube Coulomb interactions.

The momentum-dependent π plasmon frequencies are shown in Fig. 3 for the transferred momenta along the axial direction. The frequencies of the π-electronic collective excitations are higher than 6 eV even at vanishing momentum. The π plasmons in CNB's belong to optical plasmons, which behave as that of a 3D electron gas. Their frequencies depend on the transferred momenta and the nanotube radii. The

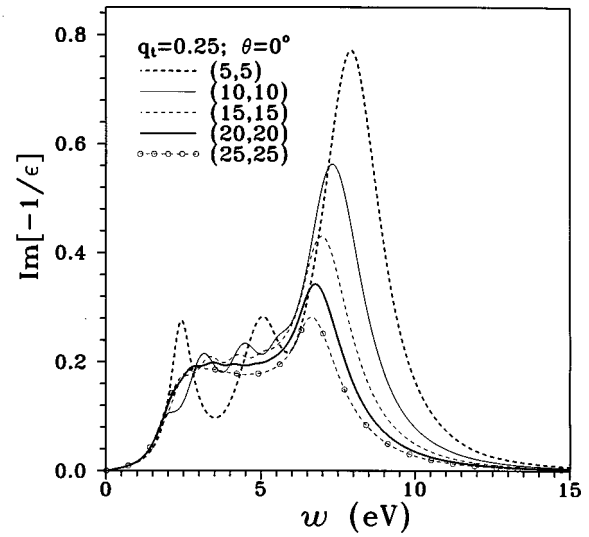

FIG. 2. The EELS of the different nanotube bundles is calculated at $q_t=0.25\ Å^{-1}$ and $\theta=0°$.

radius dependence is relatively strong at small momentum. The obvious dispersions in momenta are due to the intertube Coulomb interactions and the strong wave-vector dependence of the π band.[2–6] The π plasmon frequencies in various CNB's are $\sim 6-8$ eV at small momentum. They are close to that (~ 7 eV) of graphite.[30,31] The predicted momentum dispersions could be experimentally verified with the momentum-dependent EELS, as done for graphite.[31]

We also compare the π plasmon in a CNB with that in a single nanotube (the $L=0$ plasmon; inset in Fig. 3). In general, the frequency of the former is higher at small momenta and lower at large momenta. This result is principally determined by the 3D Coulomb interaction ($8\pi^2 e^2 N_a/q^2$) in a CNB and the 1D Coulomb interaction $[4\pi e^2 I_{L=0}(qr)K_{L=0}(qr)]$ in a single nanotube since their dielectric functions are similar to each other except the Coulomb interactions. Compared to the 1D interaction, the 3D interaction quickly diverges at vanishing q and decays at large q. The dimensionality-dependent Coulomb interactions could explain the above result.

The excitation properties, EELS, and plasmon frequencies would reflect the structure anisotropy of the CNB; that is, they alter with the direction (θ) of the transferred momentum. The EELS intensity in Fig. 4 and the plasmon frequency in Fig. 5 apparently display the anisotropic characteristic. At small q_t, the EELS intensity is stronger and the plasmon frequency is higher for smaller polar angles. The electronic excitations of the CNB at small q_t are mainly derived from the superposition of the $L=0$ and 1 excitations [Eq. (8)] of separate nanotubes. The $L=0$ excitations are stronger than the $L=1$ excitations. Moreover, the former (the latter) are the main excitations for smaller (larger) polar angles. These excitation properties could explain why the π-electronic collective excitations at small q_t become weak as θ increases. On the other hand, the $L=2$ and 3 excitations [Eq. (8)] are not negligible at large q_t. For example, the plasmon frequency for the plasma oscillation perpendicular to the axial direction is principally due to the $L=1$ excita-

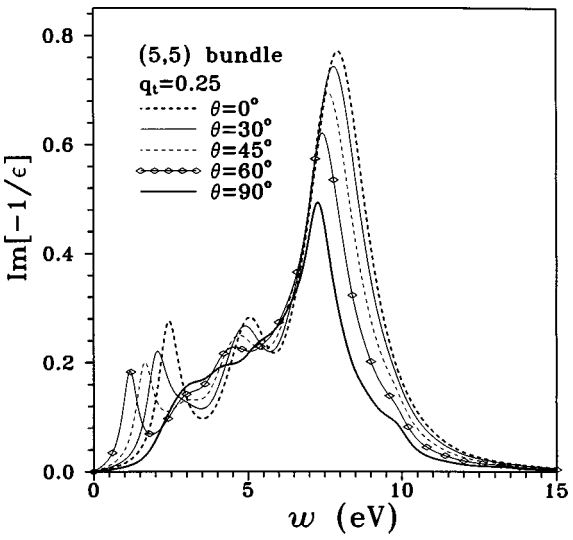

FIG. 4. Same plot as Fig. 1, but shown for the transferred momenta along the different directions and $q_t = 0.25$ Å^{-1}.

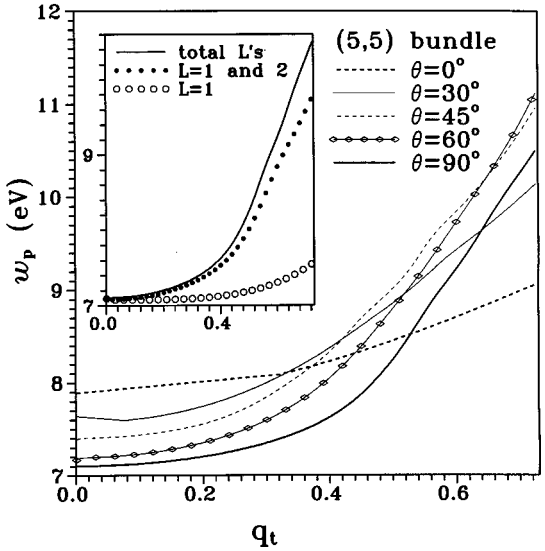

FIG. 5. Same plot as Fig. 3, but shown for the π plasmon frequencies of the (5,5) nanotube bundle in various directions.

tions at small q_t (inset in Fig. 5). However, it is significantly affected by the $L>1$ excitations at large q_t. The $L=2$ and 3 excitations would make the relatively important contribution to the dielectric response with large θ. Hence, at large q_t, there is no simple relation between the plasmon frequency (or the EELS intensity) and the polar angle, as seen in Fig. 5.

The EELS, without the momentum dependence, has been measured for a multishell nanotube[8–11] and a nanotube bundle made up of different single-shell nanotubes.[12] The π plasmon frequency is $\sim 5-7$ eV for the former and ~ 5.8 eV for the latter. The predicted $\sim(6-8)$-eV plasmon at small momentum could essentially explain the measured plasmon structures. The measurements of the momentum-dependent EELS on a uniform CNB are needed to make a more detailed comparison.

In this work we have calculated the dielectric function of the CNB within the linear-response approximation. The π-electronic excitations of the CNB are associated with those of an isolated carbon nanotube. However, they are quite different from each other, mainly owing to the intertube Coulomb coupling. The π plasmons strongly depend on the direction and the magnitude of the transferred momentum. The structure anisotropy of the CNB is directly reflected in the electronic excitations. The obvious momentum dispersions are related to the Coulomb interactions and the strong wave-vector dependence of the π band. Furthermore, the π plasmon frequencies are lower for CNB's made up of larger nanotubes. The measurements of the momentum-dependent EELS (Ref. 31) are available in verifying the predicted results. Similar studies could be generalized to understand the excitation properties of the intercalated CNB's.[26,27]

This work was supported in part by the National Science Council of Taiwan, Republic of China, under Grant Nos. NSC 87-2112-M-006-019 and 87-2112-M-009-009.

[1] S. Iijima, Nature (London) **354**, 56 (1991); S. Iijima and T. Ichihashi, *ibid.* **363**, 603 (1993); S. Iijima, P. M. Ajayan, and T. Ichihashi, Phys. Rev. Lett. **69**, 3100 (1992).

[2] J. W. Mintmire, B. I. Dunlap, and C. T. White, Phys. Rev. Lett. **68**, 631 (1992); C. T. White, D. H. Robertson, and J. W. Mintmire, Phys. Rev. B **47**, 5485 (1993).

[3] N. Hamada, S. I. Sawada, and A. Oshiyama, Phys. Rev. Lett. **68**, 1579 (1992).

[4] R. Saito, M. Fujita, G. Dresselhaus, and M. S. Dresselhaus, Appl. Phys. Lett. **60**, 2204 (1992); Phys. Rev. B **46**, 1804 (1992).

[5] H. Ajiki and T. Ando, J. Phys. Soc. Jpn. **62**, 1255 (1993); **65**, 505 (1996).

[6] X. Blase, L. X. Benedict, E. L. Shirley, and S. G. Louie, Phys. Rev. Lett. **72**, 1878 (1994).

[7] C. L. Kane and E. J. Mele, Phys. Rev. Lett. **78**, 1932 (1997).

[8] R. Kuzuo, M. Terauchi, and M. Tanaka, J. Phys. Soc. Jpn. **31**, L1484 (1992).

[9] P. M. Ajayan, S. Iijima, and T. Ichihashi, Phys. Rev. B **47**, 6859 (1993).

[10] L. A. Bursill, P. A. Stadelmann, J. L. Peng, and S. Prawer, Phys. Rev. B **49**, 2882 (1994).

[11] V. P. Dravid, X. W. Lin, Y. Wang, X. K. Wang, A. Yee, J. B. Ketterson, and R. P. H. Chang, Science **259**, 1601 (1993).

[12] R. Kuzuo, M. Terauchi, M. Tanaka, and Y. Saito, Jpn. J. Appl. Phys., Part 2 **33**, L1316 (1994).

[13] O. Sato, Y. Tanaka, M. Kobayashi, and A. Hasegawa, Phys. Rev. B **48**, 1947 (1993).

[14] P. J. Lin-Chung and A. K. Rajagopal, Phys. Rev. B **49**, 8454 (1994); J. Phys.: Condens. Matter **6**, 3697 (1994).

[15] P. S. Davids *et al.*, Phys. Rev. B **49**, 5682 (1994); **51**, 4557 (1995).

[16] B. Tanatar, Phys. Rev. B **55**, 1361 (1997).

[17] P. Longe and S. M. Bose, Phys. Rev. B **48**, 18 239 (1993).

[18] B. Vasvari, Phys. Rev. B **55**, 7993 (1997).

[19] C. Yannouleas *et al.*, Phys. Rev. B **50**, 7977 (1994); **53**, 10 225 (1996).

[20] M. F. Lin *et al.*, Phys. Rev. B **53**, 15 493 (1996); M. F. Lin and K. W.-K. Shung, *ibid.* **47**, 6617 (1993); **48**, 5567 (1993).

[21] X. K. Wang, X. W. Lin, V. P. Dravid, J. B. Ketterson, and R. P. H. Chang, Appl. Phys. Lett. **62**, 1881 (1993).
[22] W. Z. Li, S. S. Xie, L. X. Qian, B. H. Chang, B. S. Zou, W. Y. Zhou, R. A. Zhao, and G. Wang, Science **274**, 1701 (1996).
[23] Y. Saito, M. Okuda, N. Fujimoto, T. Yoshikawa, M. Tomita, and T. Hayashi, Jpn. J. Appl. Phys., Part 2 **33**, L526 (1994).
[24] A. Thess *et al.*, Science **273**, 483 (1996).
[25] C. Journet, W. K. Maser, P. Bernier, A. Loiseau, M. Lamy de la Chapelle, S. Lefrant, P. Deniard, R. Lee, and J. E. Fischer, Nature (London) **388**, 756 (1997).
[26] R. S. Lee, H. J. Kim, J. E. Fischer, A. Thess, and R. S. Smalley, Nature (London) **388**, 255 (1997).
[27] A. M. Rao, P. C. Eklund, S. Bandow, A. Thess, and R. S. Smalley, Nature (London) **388**, 257 (1997).
[28] H. Ehrenreich and M. H. Cohen, Phys. Rev. **115**, 786 (1959).
[29] For the details of the nanotube structure and the π band used in this paper see M. F. Lin and K. W.-K. Shung, Phys. Rev. B **52**, 8423 (1995).
[30] E. A. Taft and H. R. Philipp, Phys. Rev. **138**, A197 (1965).
[31] K. Zeppenfeld, Z. Phys. **243**, 229 (1971); U. Buchner, Phys. Status Solidi B **81**, 227 (1977).